Chemical Science

ROYAL SOCIETY OF CHEMISTRY

PERSPECTIVE

View Article Online
View Journal | View Issue

Check for updates

Cite this: *Chem. Sci.*, 2021, **12**, 34

All publication charges for this article have been paid for by the Royal Society of Chemistry

Received 17th September 2020
Accepted 3rd November 2020

DOI: 10.1039/d0sc05145d

rsc.li/chemical-science

Self-charging power system for distributed energy: beyond the energy storage unit

Xiong Pu *[abc] and Zhong Lin Wang *[abde]

Power devices for the smart sensor networks of Internet of things (IoT) are required with minimum or even no maintenance due to their enormous quantities and widespread distribution. Self-charging power systems (SCPSs) refer to integrated energy devices with simultaneous energy harvesting, power management and effective energy storage capabilities, which may need no extra battery recharging and can sustainably drive sensors. Herein, we focus on the progress made in the field of nanogenerator-based SCPSs, which harvest mechanical energy using the Maxwell displacement current arising from the variation in the surface-polarized-charge-induced electrical field. Prototypes of different nanogenerator-based SCPSs will be overviewed. Finally, challenges and prospects in this field will be discussed.

1. Introduction

Energy has always been critical for human civilization. It is believed that the 5G technology together with the Internet of things (IoT) and artificial intelligence will promote a new industrial revolution in the near future. However, this progress also creates new challenges for energy technologies.[1,2] Wirelessly connected sensors of the IoT, in gigantic quantities and wide geographical distribution, have to be powered with minimum or even without maintenance. Traditional electric power transmitted by long-distance cables is certainly not applicable in most cases; however, mobile electrochemical

[a]*CAS Center for Excellence in Nanoscience, Beijing Key Laboratory of Micro-Nano Energy and Sensor, Beijing Institute of Nanoenergy and Nanosystems, Chinese Academy of Sciences, Beijing 100083, China. E-mail: puxiong@binn.cas.cn*

[b]*School of Nanoscience and Technology, University of Chinese Academy of Sciences, Beijing 100049, China*

[c]*Center on Nanoenergy Research, School of Chemistry and Chemical Engineering, School of Physical Science and Technology, Guangxi University, Nanning 530004, China*

[d]*CUSPEA Institute of Technology, Wenzhou, Zhejiang, 325024, China*

[e]*School of Materials Science and Engineering, Georgia Institute of Technology, Atlanta, Georgia 30332-0245, USA. E-mail: zhong.wang@mse.gatech.edu*

Prof. Xiong Pu is an Associate Professor and principle investigator at Beijing Institute of Nanoenergy and Nanosystems (BINN), Chinese Academy of Sciences. He received his PhD Degree from the Department of Materials Science and Engineering of Texas A&M University in 2014. His research focuses on energy harvesting/storage materials and devices, triboelectric nanogenerators, self-charging power systems, and smart electronic textiles. He has published more than 60 peer-reviewed journal articles, and two chapters in related areas.

Prof. Zhong Lin Wang is the Hightower Chair in Materials Science and Engineering, Regents' Professor, and Engineering Distinguished Professor at Georgia Tech. He is also the Chief Scientist and Director for the Beijing Institute of Nanoenergy and Nanosystems, Chinese Academy of Sciences. His discovery and breakthroughs in developing nanogenerators establish the principle and technological road map for harvesting mechanical energy from environmental and biological systems for powering personal electronics. He coined and pioneered the field of piezotronics and piezo-phototronics by introducing the piezoelectric potential-gated charge transport process in fabricating new electronic and optoelectronic devices. Details can be found at: http://www.nanoscience.gatech.edu.

Open Access Article. Published on 03 November 2020. Downloaded on 07.01.26 14:11:40.
This article is licensed under a Creative Commons Attribution-NonCommercial 3.0 Unported Licence.

© 2021 The Author(s). Published by the Royal Society of Chemistry

Open Access Article. Published on 03 November 2020. Downloaded on 07.01.26 14:11:40.
This article is licensed under a Creative Commons Attribution-NonCommercial 3.0 Unported Licence.

energy storage devices require frequent battery recharging or replacement. Although portable energy storage has been powering the mobile information era with great success, it will fall short of powering the new era of IoT by itself. Alternatively, it is a promising solution to supply power to each electronic sensing node of distributed IoT networks with distributed energy harvested from its working environment.[2] However, the distributed renewable energy, including wind, solar, vibration and mechanical, are generally unstable and may vary with time, weather and location. Therefore, the integration of energy harvesting and energy storage devices becomes necessary. On one hand, the unstable electricity generated by energy harvesters can be saved and accumulated to provide a stable power supply in a certain period; on the other hand, energy storage devices may not require recharging or replacement if their power consumption is fully compensated by energy harvesters.

Self-charging power systems (SCPSs) refer to power devices integrated with energy harvesting and energy storage devices.[3] A power management circuit is also typically indispensable, which may deal with AC–DC conversion, DC–DC conversion, power matching, impedance matching, *etc.* To date, there have been attempts to integrate many different energy harvesting technologies with energy storage devices, such as solar cells, thermoelectric generators, piezoelectric nanogenerators (PENGs) and triboelectric nanogenerators (TENGs). Among these energy-harvesting technologies, PENGs and TENGs stand out for the following reasons: (i) mechanical energy resources are less dependent on weather and location; (ii) the structures and materials of these two nanogenerators are simpler and more versatile, which makes multifunctional (wearable, flexible, stretchable, *etc.*) SCPSs easier to be achieved; and (iii) human motions can not only provide power supplies but also help the realization of human–machine interactions for wearable electronics. Therefore, intensive investigations have been dedicated to developing various types of SCPS based on PENGs and TENGs, and improving their performances.

Therefore, the goal of this paper is to provide a brief review on nanogenerator-based SCPSs. As schematically shown in Fig. 1, there are generally three indispensable components in an SCPS, *i.e.* the energy-harvesting nanogenerator, rechargeable energy storage device and a power management circuit. All three aspects of SCPSs will be covered. Considering that there are several previous review papers on this topic,[3–6] this perspective will focus on updating the progress in different prototypes of SCPSs, the challenges of power management circuits, and unique requirements of appropriate energy storage devices. Finally, herein, the prospects on SCPSs are given.

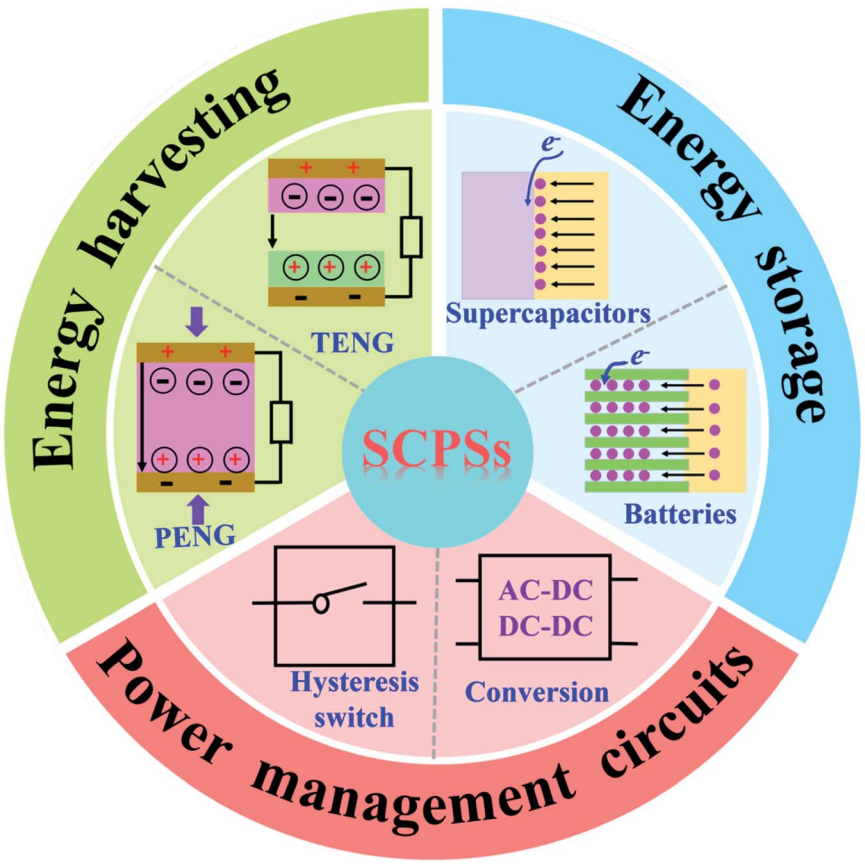

Fig. 1 Nanogenerator-based self-charging power systems (SCPC) with three components: energy harvesting, energy storage and power management circuit.

Open Access Article. Published on 03 November 2020. Downloaded on 07.01.26 14:11:40.
This article is licensed under a Creative Commons Attribution-NonCommercial 3.0 Unported Licence.

2. The evolution of nanogenerators and SCPSs

The idea of nanogenerators was first demonstrated in 2006, converting mechanical energy into electricity by deflecting ZnO nanowires with a conductive atomic force microscopy (AFM) tip in contact mode.[7] The deformation-induced strain field inside ZnO nanowires led to charge separation and a piezoelectric potential, which generated electrical current through the external circuit with the aid of rectifying Schottky contact between the AFM tip and nanowires. Meantime, the idea of self-powering was proposed.[7,8] The expectation was that an electronic system can be self-sufficient in energy if energy harvesting devices are integrated to compensate the energy consumption rather than recharging the system or using an electrical power cable. Later, the output performances and piezoelectric nanogenerators were greatly improved using horizontally aligned ZnO nanowires or ZnO nanowire/polymer composite.[9] These improvements offered opportunities to implement the idea of self-powered systems by integrating PENGs with energy storage devices. Bae *et al.* initially integrated PENGs with supercapacitors through external connections.[9–11] Xue *et al.* demonstrated the first self-charging power cell using a piezoelectric poly(vinylidene fluoride) (PVDF) separator in an LIB coin cell, which could be charged by the piezoelectric separator under pressure strain.[12]

In 2012, a flexible triboelectric nanogenerator was first invented by coupling the effects of contact electrification and electrostatic induction.[13] Subsequently, four types of fundamental modes of TENGs were developed, and their output performances were greatly improved.[14] Nanoscale or microscale morphologies on the surface of electrification layers were demonstrated to be effective in improving the output performances due to the increased effective contact areas and larger amount of accumulated electrostatic charges. Later, it was found that the fundamental theory of both PENGs and TENGs can be both unified by Maxwell's displacement current.[1] In contrast to the conventional displacement current induced by a variation in the external electrical field, a term induced by the variation of the polarization field originating from the surface polarized charges was added.[15] The displacement current J_D can be written as

$$J_D = \frac{\partial D}{\partial t} = \varepsilon \frac{\partial E}{\partial t} + \frac{\partial P_s}{\partial t} \quad (1)$$

where D is the electric displacement field, ε is the permittivity, t is time, E is the electric field, and P_s is the polarization field induced by surface polarized charges. The added term $\frac{\partial P_s}{\partial t}$ applies for both PENGs and TENGs. In PENGs, the polarization originates from the piezoelectric-induced polarization, whereas in TENGs, it is due to the surface electrostatic charges. Even though nanomaterials or nanostructures are helpful but not mandatory in TENGs, the term of nanogenerators is maintained to signify their common fundamental physics, *i.e.* surface polarized charge-induced electricity generation, and to better represent the development in this field. Due to the large output voltage of TENGs, it they have been readily integrated with energy storage devices for the purpose of self-powered systems, with several reported works showing the great potential of TENG-based self-powered systems.[16,17] Later, the term of self-charging power unit or self-charging power system was adopted for TENG-based integrated energy devices.[18] To date, the term of self-charging power system has been also widely accepted as one of the means to realize the self-powering of electronics.

3. Prototypes of nanogenerator-based SCPSs

3.1 PENG-based SCPSs

In general, two approaches have been developed to construct SCPSs based on piezoelectric nanogenerators. For the first approach, a piezoelectric film is incorporated in an electrochemical cell as the separator, the piezoelectric potential of which generated upon compressive strain can directly drive the motion of ions in the electrolyte and electrochemical reactions in the anode/cathode electrodes. Consequently, the electrochemical cells are charged without an external rectifying circuit. For the second approach, a PENG is connected to an electrochemical cell through an external rectifying circuit. The AC current of the PENG is converted into a DC current in order to charge the energy storage cell.

Xue *et al.* first demonstrated a self-charging power cell, which simultaneously completed mechanical energy conversion and electrochemical energy storage in a single coin cell (Fig. 2a).[12] A polarized piezoelectric poly(vinylidene fluoride) (PVDF) film was employed to replace the conventional polypropylene (PP) separator of a Li-ion battery (LIB). Upon compressive strain, a piezoelectric potential was generated across the PVDF film, which drove the Li ions to migrate from the cathode to anode, accompanying the Li-ion deintercalation in the $LiCoO_2$ cathode and Li-ion intercalation in the TiO_2 anode. A voltage increase from 327 mV to 395 mV in 240 s by a repeated external force of 45 N at 2.3 Hz was recorded, which also showed better charging efficiency than connecting a separate PENG to charge the battery. By using the PVDF film with opposite polarization, the piezo-electrochemical process was reversed to an accelerated discharge process due to the opposite piezoelectric-driven mitigation direction of Li ions.

Following this first proof-of-concept study, intensive efforts have been made to optimize this type of SCPS. Mesoporous PVDF membranes fabricated using ZnO NWs[19] or ZnO nanoparticles[20] as sacrificing templates were applied as the piezo-separator for better transfer of Li ions between the anodes and cathodes. Flexible batteries with a PVDF piezo-separator were also demonstrated.[21] Compared with the previous coin cells with stainless steel cases, larger strain, and therefore higher piezoelectric potential, were obtained. After applying repeated mechanical pressure of 34 N at 1 Hz for 500 s, the voltage of the Li-ion battery increased from 500 mV to 832 mV, which could deliver a discharge capacity of 0.266 μA h.[21] Flexible SCPSs also made it viable to convert mechanical input of

© 2021 The Author(s). Published by the Royal Society of Chemistry

Open Access Article. Published on 03 November 2020. Downloaded on 07.01.26 14:11:40.
This article is licensed under a Creative Commons Attribution-NonCommercial 3.0 Unported Licence.

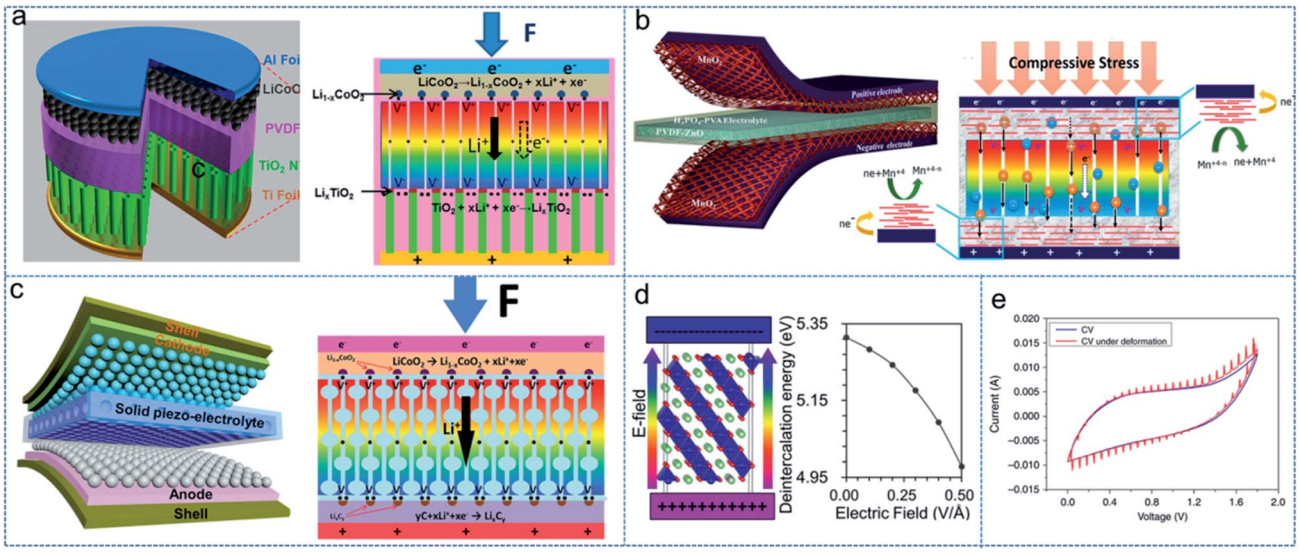

Fig. 2 Piezoelectric potential-driven self-charging power cells. (a) Structure of a self-charging power cell using a piezoelectric PVDF membrane as the separator of an LIB. Adapted from ref. 12 Copyright© 2012 the American Chemical Society. (b) Self-charging power cell using a piezoelectric PVDF/ZnO membrane as the separator of a supercapacitor. Adapted from ref. 39 Copyright© 2015 the American Chemical Society. (c) Self-charging power cell using a solid piezo-electrolyte of an LIB. Adapted from ref. 32 Copyright© 2017 Elsevier. (d) Simulation showing the lowered deintercalation energy of the Li ions in the electrode by the piezoelectric potential. Adapted from ref. 43 Copyright© 2017 the American Chemical Society. (e) Cyclic voltammetry curve of a self-charging cell tested under intermittent compressive deformation. Adapted from ref. 40 Copyright© 2020 Springer Nature Limited.

bending and stretching into electrochemical responses.[22,23] Composite piezo-separators incorporated with inorganic piezoelectric materials with a higher piezoelectric coefficient were also investigated to improve the performances, such as lead zirconate titanate (PZT),[24] potassium sodium niobite (KNN),[23,25] $NaNbO_3$,[26] $0.5(Ba_{0.7}Ca_{0.3})TiO_3$–$0.5Ba(Zr_{0.2}Ti_{0.8})O_3$ (BCT–BZT) nanofibers,[27] and ZnO.[28–30] Self-polarized piezoelectric biomaterials, *e.g.* perforated fish swim bladder, were also demonstrated as efficient piezo-separators.[31] Recently, piezoelectric materials were further incorporated into a solid electrolyte, resulting in a piezo-electrolyte, which can provide the piezoelectric potential and function simultaneously as the separator and electrolyte of electrochemical cells (Fig. 2c).[32] This type of piezo-electrochemical process has also been demonstrated to be applicable to electrochemical double layer (EDL) supercapacitors (Fig. 2b),[33–37] pseudocapacitive supercapacitors,[31,38–42] and sodium ion batteries.[25]

Wang *et al.* provided a density functional theory (DFT) simulation to understand the mechanism of the piezo-electrochemical process in this type of SCPS (Fig. 2d).[43] According to their findings, the piezoelectric field can reduce the intercalation and deintercalation energies of cathode and anode materials during the self-charging process, respectively. Meantime, it can also lead to a decrease in the diffusion barriers of Li ions. Recently, Krishnamoorthy *et al.* proposed a piezo-electrochemical spectroscopy measurement to probe the self-charging process of an SCPS with siloxene as the capacitive active material.[40] Cyclic voltammetry was performed when pressure was applied repeatedly. Upwards current spikes were observed above the zero charge region, while the polarity of the current spikes was opposite below the zero charge region (Fig. 2e). These observations confirmed the piezo-electrochemical processes in the SCPS. Furthermore, the amplitude of the current spikes was related to the state of charge (SOC) of the electrochemical cell, which provided dynamic information of the electrochemical responses to the piezoelectric potentials.

The second approach of PENG-based SCPSs is to connect a PENG and an energy storage device through an external circuit. The benefits of the first approach include the simplicity of the whole structure and high self-charging efficiency. However, the voltage increment of electrochemical cells is limited by the piezoelectric potential. Generally, the voltage can only increase several hundreds of millivolts, which is not sufficient to provide a sustainable power supply to self-powered electronics. In the case of the second approach, the PENG and energy storage devices (batteries or supercapacitors) are constructed separately. The open-circuit voltage of a PENG has been reported to be about ~10 V,[11] which theoretically can fully charge a battery or supercapacitor cell (typically less than 5 V) if the charge quantity extracted from the PENG in a certain period is sufficient.

Zhu *et al.* reported a PENG with lateral ZnO NW arrays, which was connected to commercial capacitors through a rectifying circuit.[9] The PENG output an open-circuit voltage of 2.03 V and peak power density of ~11 mW cm^{-3}. The capacitors were charged by the PENG in parallel connection, and then reconfigured into series connection for lighting up a red LED. Hu *et al.* proposed a self-powered system with a PENG-based SCPS as the power source for sensors, data processors and transmitters.[11] A PENG outputting a voltage of 10 V and current of 0.6 μA was demonstrated to be able to charge a 22 μF capacitor,

Open Access Article. Published on 03 November 2020. Downloaded on 07.01.26 14:11:40.
This article is licensed under a Creative Commons Attribution-NonCommercial 3.0 Unported Licence.

which then powered a radio frequency transmitter (<1 mW power consumption). This work first demonstrated a self-powered system powered by PENG-based SCPSs for wireless data communication. Recently, Qin's group reported a 3D intercalation electrode-based PENG using a piezoelectric material with high piezoelectric coefficient (Sm-PMN-PT), which achieved a record-high current density of 290 μA cm^{-2} and surface charge density of 1.69 mC m^{-2}.[44] Based on this PENG, the SCPS could charge a 1 μF capacitor from 0 V to 8 V in 21 cycles of motion.

In summary, the two approaches for PENG-based SCPSs both have advantages and disadvantages. In the case of the first approach using "intrinsic" self-charging cells, the advantages include simple cell structure, facile operation mode and high charging efficiency, but the self-charged voltage (ΔV) is still limited. For this type of SCPS, future research may need to focus on methods to improve the self-charged voltage increment. For the second approach using "extrinsic" self-charging systems, the advantage is that the electrochemical energy storage cells can be fully charged theoretically. The disadvantages include the complicated structure and difficulty to achieve fully flexible/stretchable systems if the management circuits are considered. Another issue of the second approach is the low charging efficiency and low charging rate. This is partially due to the low output of PENGs and partially due to the impedance mismatch between PENGs and batteries/supercapacitors. These issues are very similar to the TENG-based SCPSs discussed subsequently in Section 4. Some of the power management circuits proven to be effective for TENG-based SCPSs can actually also be investigated in the future for PENG-based SCPSs, such as the switched-capacitor step-down circuit discussed subsequently in Section 4.

3.2 TENG-based SCPSs

TENGs typically output pulsed AC electricity with high voltage, low current and large internal impedance. Several strategies have recently been developed to realize DC current, but their electrical outputs are still pulsed.[45–47] To apply TENGs as a power source of electronics, there are generally two

Table 1 Representative performances of TENG-based SCPSs[a]

TENG	Energy storage devices	Output of TENG	Performance of SCPSs	Reference
Arch-shaped C-S TENG	LIBs (~20 μA h)	V_{oc} = 225 V, I_{sc} = 140 μA	0.7 V to 2.5 V in 11 h	17
Textile TENG	Flexible belt-shaped LIBs	V_{oc} = 52 V, I_{sc} = 3.5 μA	0.4 V to 1.9 V in 4 h	18
C-S mode TENG	Flexible LIBs (104 mA h g^{-1})	V_{oc} = 200 V, I_{sc} = 25 μA	1.5 to 3.5 V in 3 min	82
C-S mode TENG	LIBs	V_{oc} = 188 V, I_{sc} = 33.5 μA	0.5 to 3 V in 8 min	83
Flexible C-S mode TENG	Flexible solid LIBs	V_{oc} = 135 V, I_{sc} = 12 μA	1.5 to 3.5 V in 55 s	81
F-S fabric TENG	Fiber supercapacitors (2.25 mF cm^{-1})	V_{oc} = 118 V, I_{sc} = 1.5 μA	0 to 1.5 V in 2400 s	55
PET yarn-based C-S TENG	Yarn-based supercapacitors (78.1 μW h cm^{-2})	V_{oc} = 60 V, I_{sc} = 4 μA	0 to 2.4 V in 104 min	56
Fabric-based C-S TENG	rGO-based textile supercapacitors (2.1 mF)	V_{oc} = 50 V, I_{sc} = 2 μA	0 to 2 V in 34 min	57
Paper-based C-S TENG	Paper-based supercapacitor (~2 mF)	V_{oc} = 110 V, Q_{sc} = 750 nC	0 to 25 mV in 15 s	63
Flexible S-E mode TENG	Commercial supercapacitor (22 μF)	V_{oc} = 200 V, I_{sc} = 20 μA	0 to 2 V in 750 s	68
Transparent S-E mode TENG	A transparent and flexible supercapacitor (1.3 mF cm^{-2})	V_{oc} = 30 V, I_{sc} = 0.2 μA	0 to 2.5 V within 6102 s	70
Cotton cloth-based TENG	Textile based solid-state rGO supercapacitors (13 mF cm^{-1})	V_{oc} = 40 V, I_{sc} = 5 μA	0 to 2.1 V in 913 s	51
Flexible C-S TENG	Fabric supercapacitors (16.76 mF cm^{-2})	V_{oc} = 200 V, I_{sc} = 100 μA	0 to 100 mV in 6 min	61
Flexible C-S TENG	Solid-state fiber-shaped supercapacitors (2.5 F cm^{-3})	—	0 to 2.4 V in 5 s	16
Hydraulic C-S TENG	Fiber supercapacitors (4 F cm^{-3})	V_{oc} = 100 V, I_{sc} = 200 μA	0 to 4 V in 55.7 s	80
Flexible C-S mode TENG	Transparent and flexible supercapacitor (3.83 μF cm^{-2})	V_{oc} = 135 V, I_{sc} = 43 μA	0 to 0.5 V in 20 s	71
Stretchable TENG	Stretchable supercapacitors	V_{oc} = 120 V, Q_{sc} = 90 nC	0.13 to 0.16 V in 60 s	67
Flexible S-E mode TENG	Flexible kirigami paper based supercapacitor	V_{oc} = 250 V, Q_{sc} = 160 nC	0 to 1.3 V in 90 s	72
Flexible S-E mode TENG	Solid-state microsupercapacitor	V_{oc} = 50 V, I_{sc} = 0.12 μA cm^{-2}	0 to 0.15 V in 200 s	77
Flexible C-S mode TENG	Flexible asymmetric supercapacitor (155.8 F g^{-1})	V_{oc} = 200 V, I_{sc} = 30 μA	0 to 1.2 V in 900 s	74

[a] C-S: contact-separation, S-E: single-electrode, F-S: free-standing.

© 2021 The Author(s). Published by the Royal Society of Chemistry

Open Access Article. Published on 03 November 2020. Downloaded on 07.01.26 14:11:40.
This article is licensed under a Creative Commons Attribution-NonCommercial 3.0 Unported Licence.

approaches, *i.e.* high voltage source and integrated SCPS.[48,49] The first approach allows the possible utilization of a TENG without a management circuit and facilitates the realization of simple structures of self-powered systems.[50] The second approach aims to accumulate the unstable electricity of the TENG and supply stable power for electronics for a certain period. Obviously, the latter strategy is suitable for more applications since most electronics require a stable electricity supply with a voltage of less than about 5 V. This section will briefly introduce the representative prototypes of TENG-based SCPSs for wearable electronics. Emphasis will be put on the attempts to improve their multifunctionality and integration level, while SCPSs using commercial capacitors or batteries will not be included. Table 1 summarizes some of the representative TENG-based SCPSs.

Wearable TENG-based SCPSs targeted for applications in smart textiles are of great interest in recent times. The rigidity and limited power of conventional batteries make them unsuitable for smart electronic textiles. On the contrary, TENGs in the shape of fibers, yarns, threads, and woven or knitted textiles have been widely reported with demonstrated flexibility, stretchability, and even washability. Therefore, it is promising for a sustainable or self-powered electronic textile to combine textile-based TENGs with flexible energy storage devices. Xiao *et al.* constructed an SCPS with solid-state fiber-shaped supercapacitors charged by a flexible TENG (Fig. 3a(i)).[16] Three

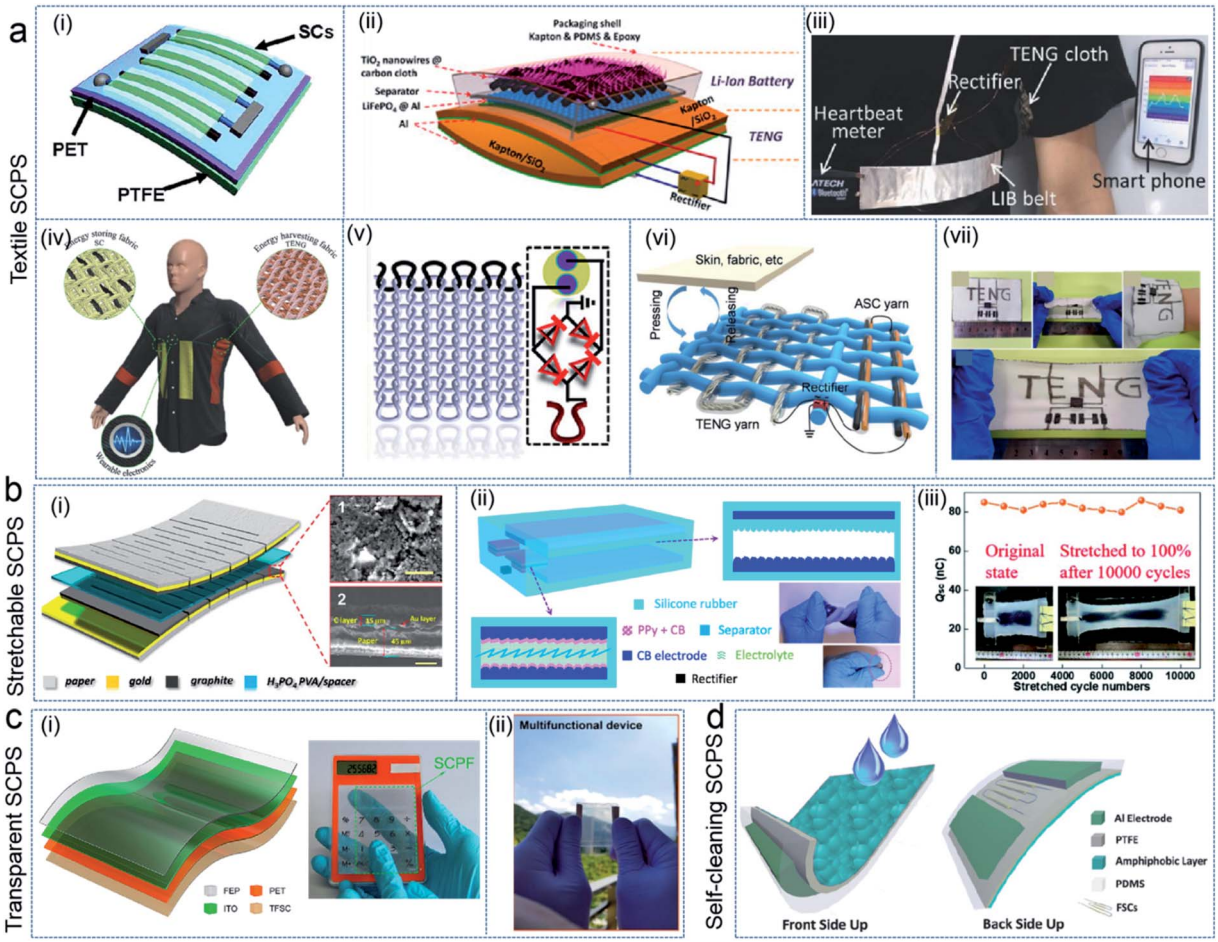

Fig. 3 TENG-based SCPSs. (a) Textile-based SCPSs. (i) SCPS using fiber-based solid supercapacitors as the energy storage. Adapted from ref. 16 Copyright© 2012 the American Chemical Society. (ii) Motion-charged SCPS with textile-based LIB. Adapted from ref. 17 Copyright© 2013 the American Chemical Society. (iii) SCPS with a textile-based TENG and flexible belt-type LIB. Adapted from ref. 18 Copyright© 2015 John Wiley & Sons, Inc. (iv) Scheme of an all-textile-based SCPS. Adapted from ref. 51 Copyright© 2016 John Wiley & Sons, Inc. (v) Stretchable textile-based SCPS. Adapted from ref. 53 Copyright© 2017 the American Chemical Society. (vi) SCPC with yarn-type TENG and yarn-type asymmetric supercapacitors. Adapted from ref. 56 Copyright© 2019 John Wiley & Sons, Inc. (vii) Stretchable coplanar textile-based SCPS. Adapted from ref. 57 Copyright© 2020 the American Chemical Society. (b) Stretchable SCPSs. (i) Kirigami paper-based supercapacitor for stretchable SCPS. Adapted from ref. 72 Copyright© 2016 the American Chemical Society. (ii) Stretchable SCPS with elastomer silicone rubber as the substrate. Adapted from ref. 67 Copyright© 2016 the American Chemical Society. (iii) Stretchable SCPS using liquid PEDOT:PSS as the electrode. Adapted from ref. 68 Copyright© 2019 The Royal Society of Chemistry. (c) Transparent SCPSs. (i) Transparent SCPS using ITO as the electrode in a TENG and microsupercapacitors as the energy storage. Adapted from ref. 70 Copyright© 2016 the American Chemical Society. (ii) Transparent SCPS using graphene as the electrode in both the TENG and supercapacitors. Adapted from ref. 71 Copyright© 2019 the American Chemical Society. (d) Self-cleaning SCPS with an amphiphobic layer. Adapted from ref. 80 Copyright© 2018 John Wiley & Sons, Inc.

Open Access Article. Published on 03 November 2020. Downloaded on 07.01.26 14:11:40.
This article is licensed under a Creative Commons Attribution-NonCommercial 3.0 Unported Licence.

supercapacitors connected in series could be charged to 2.4 V in 5 s by the TENG, which could then power a commercial liquid crystal display (LCD) and light-emitting diode (LED). Wang *et al.* reported an integrated flexible SCPS by combing an arch-shaped TENG with an Li-ion battery using carbon cloth as conductive current collectors (Fig. 3a(ii)).[17] A rectifier was connected in the circuit to convert the AC current of the TENG into DC current. In the "standby mode", the LIB could be fully charged from 0.7 V to 2.5 V in ~11 h with a mechanical motion at about 9 Hz, which could then provide about ~20 μA h discharge capacity. In "sustainable mode", the SCPS could provide a constant current of 2 μA at the voltage of 1.55 V for more than 40 h. Pu *et al.* initially developed an SCPS with fabric-based TENGs (Fig. 3a(iii)).[18] Conductive Ni thin coatings and dielectric parylene films prepared conformally on polyester fabrics were employed as the electrodes and electrification layers for a woven textile-shaped TENG, respectively. A flexible belt-shaped LIB was fabricated to store the energy harvested by the textile TENG. The textile TENG was demonstrated to be able to harvest energies of different types of human motions. When charging the LIB belt with the textile TENG working at a contact-separation motion mode with 0.7 Hz frequency for 14 h, the delivered corresponding discharge capacity reached 4.4 mA h cm^{-2} at a discharge current of 1 μA. Later, this team proposed an all-textile-based SCPS integrated with textile TENGs and yarn supercapacitors (Fig. 3a(iv)).[51] The solid-state supercapacitors utilized reduced graphene oxide (rGO) as the EDL capacitive active material and 1D Ni-coated yarn as the current collector, achieving a capacitance of 13 mF cm^{-1}. They demonstrated the potential of weaving the textile TENGs and yarn supercapacitors into a single piece of fabric. Three supercapacitors connected in series could be charged to 2.1 V in 913 s with 10 Hz mechanical motions, which then delivered 1 μA constant current for 808 s. Wang *et al.* also demonstrated an SCPS with fiber-shaped solid-state supercapacitors charged by fiber TENGs.[52] Afterwards, a series of different prototypes of SCPSs was reported based on fiber-, yarn- and fabric-based supercapacitors and TENGs.[53–60] Dong *et al.* realized a stretchable all-yarn-based SCPS based on knitting fabrics (Fig. 3a(v)).[53] The stretchability originated from the intrinsic feature of the knitting structures, and the TENG fabric was also demonstrated to be washable. Song *et al.* reported an all-fabric-based SCPS, where the fabric supercapacitors showed an areal capacitance of 16.76 mF cm^{-2} and could be charged to 100 mV during running motion in 6 min.[61] Chen *et al.* realized sliding-mode TENGs with interdigitated electrodes by traditional weaving methods, and demonstrated a one-piece SCPS textile using fiber supercapacitors as the energy storage unit.[55] The SCPS showed a charging rate of 1.4 μC s^{-1} at 1.5 Hz rubbing motions. Liu *et al.* reported a yarn-based SCPS using high-energy asymmetric supercapacitors as the energy storage unit (Fig. 3a(vi)).[56] Fluorination surface modification was conducted on the TENG textile to enhance the triboelectrification and output performances, and the asymmetric supercapacitors showed a high energy density of 78.1 μW h cm^{-2}. Cong *et al.* also reported a stretchable SCPS fabricated on a single piece of fabric by a resist-dyeing method, where both the textile TENG and in-plane supercapacitors were highly stretchable (Fig. 3a(vii)).[57]

Considering that the contact-electrification phenomenon is universal for almost all types of materials and the structure of TENGs is relatively simple, TENGs can be fabricated based on many different materials and different functionalities can be realized. Besides textiles, SCPSs were also reported based on paper,[62–65] plastic,[66] elastomeric polymer,[67–69] *etc.* Furthermore, multifunctional SCPSs have also been widely reported, including transparent,[70,71] flexible, and stretchable SCPSs.[57,67–69] In these multifunctional SCPSs for wearable electronics, supercapacitors have been frequently employed as the energy storing unit because compared to batteries, they are easier to realize comparable transparency, flexibility, and stretchability. Supercapacitors with a stacked configuration[61,67,71–76] or in-plane microsupercapacitors[57,70,77–79] were reported in these devices. For example, Guo *et al.* reported a stretchable SCPS based on a shape-adaptive supercapacitor with a kirigami paper architecture (Fig. 3b(i)),[63,72] while several other works reported stretchable SCPSs using elastomeric polymers as the substrates and electrification layers in the TENG (Fig. 3b(ii)).[67,68] A transparent SCPS was reported for a smart sliding unlock touchpad using an ITO electrode in the TENG and interdigitated Au/MnO_2 electrodes in the microsupercapacitors (Fig. 3c(i)).[70] A transparent SCPS was also reported using single-layer graphene as the electrodes in both the TENG and supercapacitors (Fig. 3c(ii)).[71] Zhang *et al.* reported a self-cleaning SCPS, which harvested and stored energy from falling raindrops (Fig. 3d).[80] Amphiphobic PTFE was used as the tribo-electrification layer, which could generate static charges when directly contacting with water drops. In general, it is facile for the TENG to realize these multifunctionalities. The difficulties for realizing multifunctional SCPSs originate from two aspects, *i.e.* the energy storage unit, which involves slightly more complicated structures and materials; and the rectifying circuit, which may not be flexible. In the case of the former, it may be hard for alkaline metal-ion batteries using an organic electrolyte to realize multifunctional SCPSs, but aqueous secondary batteries (such as Zn ion batteries) should be good alternatives to supercapacitors considering their higher energy density. However, SCPSs using aqueous batteries are rarely reported. For the latter, half-wave diodes or full-wave bridge rectifiers were used in almost all the reports and no better solution has been proposed thus far.

Efforts have also been made to improve the integration level of the SCPSs. Although it is hard to integrate the TENG and energy storage device with shared electrodes, SCPSs with a shared package or substrate have been reported.[17,61,72,81–83] The TENG and batteries/supercapacitors can be designed on the same substrate, or the electrification layer and/or electrode of the TENG can serve as the package of the batteries/supercapacitors. For example, an all-in-one SCPS was reported with the electrification layers and electrodes of two TENGs attached on the top and bottom side of a supercapacitor.[61] Zhao *et al.* attempted to design SCPSs where static charges can directly induce charges in the current collectors of LIBs, and therefore charge flow between the battery electrodes.[82] A wind-

© 2021 The Author(s). Published by the Royal Society of Chemistry

Open Access Article. Published on 03 November 2020. Downloaded on 07.01.26 14:11:40.
This article is licensed under a Creative Commons Attribution-NonCommercial 3.0 Unported Licence.

driven FEP membrane vibrated between two LIB pouch cells, the sealing polymer of which could function as the electrification layer of the TENGs. Charges were claimed to be electrostatically induced directly in the current collectors of the LIB. The LIB was demonstrated to be charged to 3.5 V in 3 min by wind-driven vibration energies. Another work designed an SCPS where the electrification occurred inside an LIB cell with a solid-state electrolyte, and relative motions between the anode and cathode caused electrostatic induction in the current collectors.[83] Nevertheless, the electrochemical performances of the battery deteriorated due to the increased contact impedance in the cell.

3.3 Hybrid SCPSs

Considering that different renewable energy resources all have limitations, hybrid energy-harvesting devices may be an effective approach to combine the advantages of each unit. To date, a variety of combinations of different energy harvesting devices have been integrated together for simultaneously scavenging different energies.[84] For example, TENGs have been demonstrated to be highly efficient for harvesting mechanical energies at low frequency, whereas conventional electromagnetic generators (EMG) have larger efficiency for mechanical energies with high frequency. Therefore, the combination of TENGs and EMGs could harvest mechanical energies of wide-band frequencies.[85,86] TENGs and PENGs have also been integrated together to improve their output performances. Solar cells and thermoelectric generators had been reported to be integrated with TENGs and PENGs to harvest solar energy and thermal energy, respectively.[87] Yang *et al.* reported a series of works combining PENGs or TENGs with one or two other energy harvesting techniques, including pyroelectric nanogenerators, thermoelectric generators and solar cells.[84,88–92] Recently, a biofuel cell was reported to be integrated with a TENG also.[93]

SCPSs have been reported with two or more energy-harvesting devices integrated together. Generally, different energy-harvesting units are connected with the TENG or PENG in parallel connection. These hybrid energy-harvesting units make the corresponding SCPSs applicable in more environments with higher performances. In 2011, Bae *et al.* reported a fiber-shaped SCPS, which integrated a ZnO NW-based PENG, a solar cell, and a supercapacitor in a single fiber.[10] The ZnO NWs grown on a carbon fiber functioned simultaneously as the photoelectrode in the solar cell, piezoelectric materials in the PENG, and active materials in the supercapacitor. Another work also fabricated a hybrid SCPS on a single optical fiber.[87] The inner core was a dye-sensitized solar cell (DSSC) with ZnO NWs grown on ITO as the photoelectrode, and the outer sheath was a ZnO NW-based PENG. The photon transferred inside the optical fiber and bending motions of the fiber could be converted into electricity. Qin *et al.* reported an SCPS with a PENG and TENG integrated together with microsupercapacitors (Fig. 4a).[94] A PENG with PVDF–TrFE as the piezoelectric material was stacked with a TENG working at contact-separation mode, and the electrochromic microsupercapacitors utilized Ag NWs and NiO as the electrode materials. The hybrid nanogenerators outputted a voltage of 150 V and a current of 20 μA, and the integrated microsupercapacitor array was capable of self-charging to 3 V to light up an LED under human palm impact. Recently, Zhang *et al.* reported a bracelet incorporated

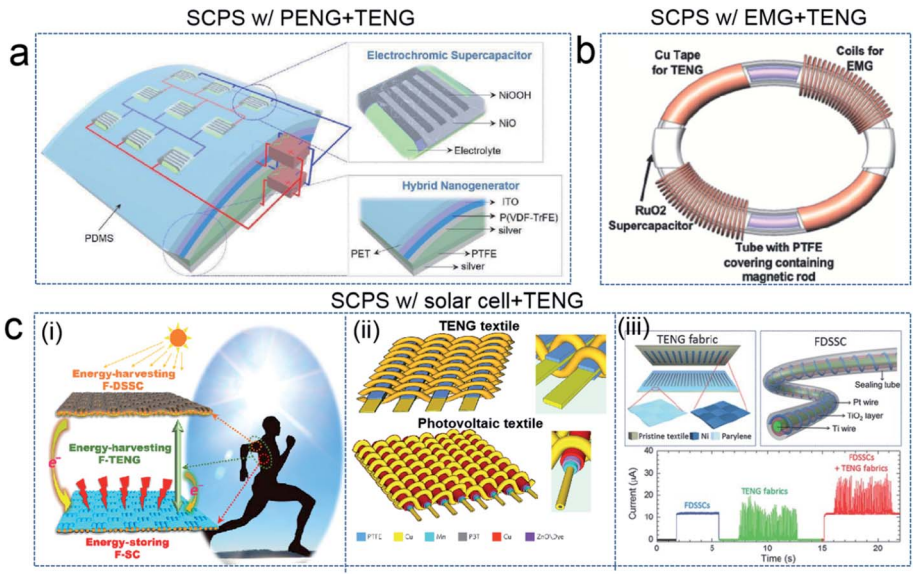

Fig. 4 Hybrid SCPSs. (a) SCPS hybrid with a TENG and PENG for mechanical energy harvesting. Adapted from ref. 94 Copyright© 2018 John Wiley & Sons, Inc. (b) Bracelet-shaped SCPS hybrid with an electromagnetic generator (EMG) and TENG for energy harvesting. Adapted from ref. 79 Copyright© 2019 John Wiley & Sons, Inc. (c) SCPSs hybrid with solar cells and TENGs for energy harvesting. (i) All-fiber-based SCPS with fiber DSSCs, fiber TENGs and fiber supercapacitors. Adapted from ref. 95 Copyright© 2016 American Association for the Advancement of Science. (ii) Energy-harvesting textile with TENG textile for mechanical energy harvesting and solid-state photovoltaic textile for solar energy harvesting. Adapted from ref. 96 Copyright© 2016 Springer Nature Limited. (iii) Energy-harvesting textile with sliding-mode TENG textile and fiber-shaped DSSCs. Adapted from ref. 97 Copyright© 2016 John Wiley & Sons, Inc.

Open Access Article. Published on 03 November 2020. Downloaded on 07.01.26 14:11:40.
This article is licensed under a Creative Commons Attribution-NonCommercial 3.0 Unported Licence.

with microsupercapacitors, which were self-charged by a TENG and an EMG with energy converted from hand gestures (Fig. 4b).[79] A PTFE tubular bracelet was wrapped with RuO_2-based microsupercapacitors, two Cu electrodes for the TENG and two coils for the EMG. The sliding motion of the two Cu cylinders inside the bracelet led to the generation of electricity in the TENG electrodes and EMG, which was then stored in the microsupercapacitors. The SCPS was charged to 2 V with a single shake of the human wrist, allowing it to power most electronic devices for minutes. SCPSs integrating TENGs with solar cells have also been reported. Wen *et al.* also developed a textile-based SCPS integrating TENGs, solar cells and supercapacitors all in a fiber shape (Fig. 4c(i)).[95] The fiber DSSC showed an efficiency of 5.64%, and the TENG output a current of ~0.91 μA when jogging. The fiber supercapacitors could be charged to 1.8 V in 69 s by the hybrid energy harvesting textiles. Chen *et al.* further proposed a hybrid energy harvesting textile integrated with all-solid-state DSSC fabrics and TENG fabrics (Fig. 4c(ii)).[96] The photoelectrode wire and Cu counter electrode were woven into a DSSC fabric without using liquid electrolyte. A 2 mF capacitor could be charged for 1 min and then power different electronics. Pu *et al.* reported a self-charging power textile integrated with fiber DSSCs and TENG fabric, which could charge an LIB coin cell for 10 min, and later be discharged at 1 μA for 98 min (Fig. 4c(iii)).[97]

4. Power management circuit

The power management circuit is of significance for nanogenerator-based SCPSs. This section will focus only on the power management circuit for TENG-based SCPS since it has been intensively investigated recently. TENGs generally output high voltage (tens to thousands of volts) and low current (μA level) with a very large internal impedance of around 10^5 to 10^7 ohm. Nevertheless, the energy storage units, *i.e.* supercapacitor or battery cells, typically work at an operational voltage of lower than 5 V and require a large current (mA level) to be fully charged. Meantime, the internal impedance of the energy storage cell is typically smaller than 100 ohm level (depending on the capacity of the cell). The output power of the TENG will be maximized when the external load impedance is close to its internal impedance, and thus the energy extracted from the TENG will be low when directly charging the battery or supercapacitor cell with a bridge rectifier. Therefore, a power management circuit is highly necessary to bridge the gap between the nanogenerators and energy storage units.[98] Furthermore, it is also demonstrated that appropriate design of the management circuit is effective in improving the output performances of the TENG itself.[99,100] A recent paper provided a relatively comprehensive review on power management circuits for TENGs.[101,102] Here, a brief discussion will be given with an introduction on the updated progress.

To improve the charging efficiency of SCPSs, the power management circuit for a TENG should generally include the following parts: (i) an AC–DC converter, (ii) a voltage step-down converter, and (iii) a hysteresis switch to maximize the *V*–*Q* plot area per motion cycle (*i.e.* the extracted energy per cycle). The AC–AC voltage drop can be achieved by an inductor transformer, which, however, applies well only to rotational TENGs with sinusoidal output but not TENGs with intermittent pulsed output.[98] Alternatively, DC–DC converters can be utilized after the AC–DC conversion. Therefore, a universal management circuit typically has the three stages, as shown in Fig. 5a. In the first stage, the AC output of the TENG is converted to a DC output with rectifiers. In most works, full-wave bridge rectifiers have been utilized (Fig. 5b(i)). Nevertheless, the half-wave rectifier (Fig. 5b(ii)) and Bennet's doubler conditioning circuit (Fig. 5b(iii)) were recently reported to increase the rectified DC voltage.[102–104] Especially, Basset's group demonstrated that Bennet's doubler can output a much larger DC energy per cycle than the other two rectifying circuits.[103] A buffering capacitor (C_{buff}) with comparable capacitance to that of the TENG was typically connected after the rectifying circuit.

For the second stage, a hysteresis switch is crucial to maximize the extracted energy from the TENG according to the *V*–*Q* plot of the TENG in each motion cycle.[105] This strategy was first demonstrated by Zi *et al.* (Fig. 5c(i)).[106] Different methods were later proposed to realize this switch. Mechanical switches were firstly used, but they were not autonomous and not convenient for practical applications. Cheng *et al.* reported an electrostatic vibrator switch driven by the TENG itself.[107] Recently, Basset's group reported a microelectromechanical system (MEMS) plasma switch to fulfill this function (Fig. 5c(ii)).[108] Xi *et al.* utilized a metal-oxide-semiconductor field-effect transistor (MOSFET) and a comparator for this purpose (Fig. 5c(iii)).[109] When the rectified voltage is larger than the reference voltage of the comparator (typically preset according to the maximum voltage of the TENG), the transistor switch is open, and thus the extracted energy is maximized.

For the third stage, a DC–DC converter is employed for stepping down the voltage. Different approaches have been reported. Niu *et al.* and Cheng *et al.* reported the utilization of an inductive transformer for the voltage drop (Fig. 5d(i)).[110,111] Later, a conventional DC–DC bulk convertor, consisting of a parallel freewheeling diode, a serial inductor and a parallel capacitor, was adopted in several different works (Fig. 5d(ii)).[108,109,112] Different from these converters with inductors, capacitive transformers have also been reported for stepping down the voltage. In general, a certain number of capacitors are connected in series when being charged and then switched to parallel connection when discharging. Accordingly, the output voltage is lowered, and the output charge quantities are the sum of these capacitors. Tang *et al.* and Zi *et al.* first tried this strategy for TENG conditioning circuits, respectively.[113,114] Recently, Liu *et al.* further reported a fractal design-based capacitive convertor (Fig. 5d(iii)).[115] Rectifying diodes were utilized to realize the automatic switch between the series and parallel connection of the capacitors. Meantime, the fractal design could reduce the number of necessary diodes, leading to a lower total voltage loss across all the diodes. Over 94% energy transfer efficiency was then achieved. After the DC–DC conversion, the output could be connected to a regulator for a stabilized constant voltage supply to the external electronics. Commercial regulators can be utilized or a storage capacitor can

© 2021 The Author(s). Published by the Royal Society of Chemistry

Open Access Article. Published on 03 November 2020. Downloaded on 07.01.26 14:11:40.
This article is licensed under a Creative Commons Attribution-NonCommercial 3.0 Unported Licence.

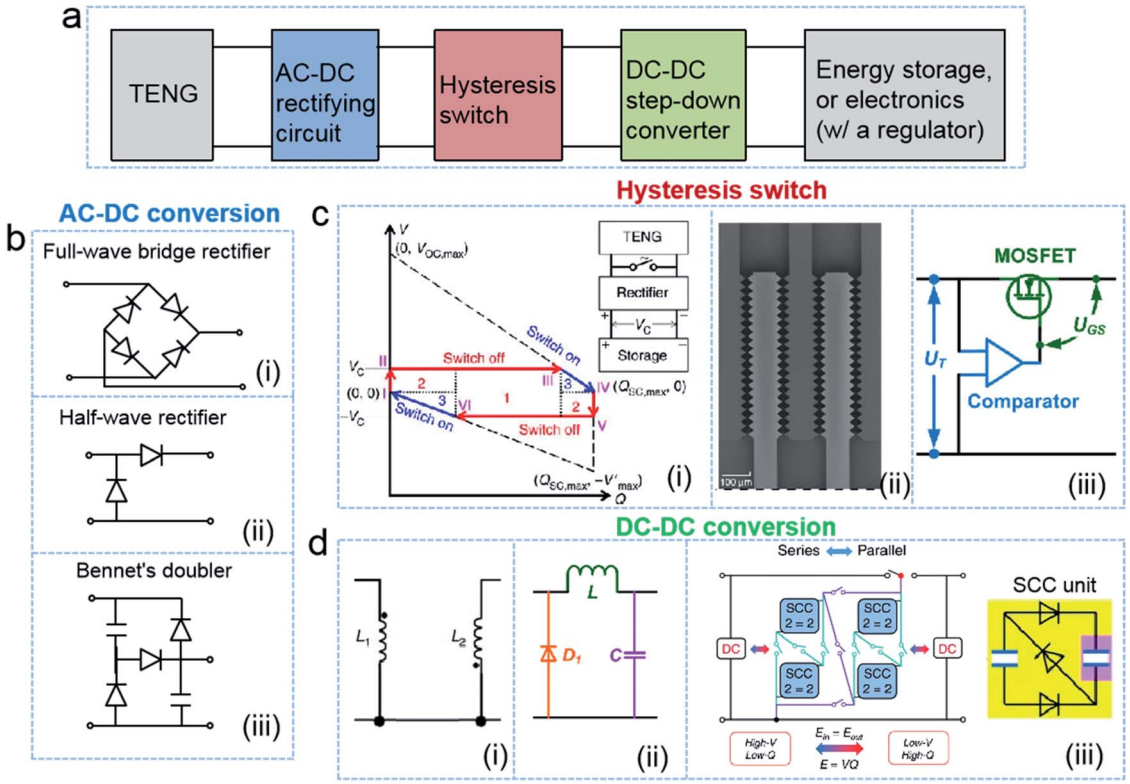

Fig. 5 Power management for TENG-based SCPSs. (a) Typical universal circuit for TENG-based power management circuits. (b) Typical AC–DC conversion circuits. (i) Full-wave bridge rectifying circuit. (ii) Half-wave rectifying circuit. (iii) Bennet's doubler conditioning circuit. (c) Typical strategies for the hysteresis switch. (i) Maximizing the V–Q plot area of a TENG in a single motion cycle by a mechanical switch. Adapted from ref. 106 Copyright© 2016 Springer Nature Limited. (ii) Automatic approach using an MEMS plasma switch. Adapted from ref. 108 Copyright© 2020 Springer Nature Limited. (iii) Automatic switch based on a MOSFET and a comparator. Adapted from ref. 109 Copyright© 2017 Elsevier. (d) Typical DC–DC conversion circuits. (i) Inductor-based DC–DC conversion circuit. Adapted from ref. 110 Copyright© 2015 Springer Nature Limited. (ii) LC circuit for DC–DC conversion. Adapted from ref. 109 Copyright© 2017 Elsevier. (iii) Switched capacitor-based conversion (SCC) circuit with fractal designs. Adapted from ref. 115 Copyright© 2020 Springer Nature Limited.

be directly connected for constant power supply to electronics. According to the two separate works of Xi *et al.* and Liu *et al.*, continuous operation of a series of small electronics could be constantly powered by a TENG with power management circuits, including a thermometer, pedometer, electronic watch, calculator, buzzer, and temperature hygrometer.[109,115]

5. Energy storage for SCPSs

The majority of TENGs output an intermittent DC current after AC–DC conversion. The rectified sliding-mode TENG can output a sinusoidal-ripple current. Even if a power management circuit is applied to generate a constant voltage, the mechanical energy input may still not be continuous. Therefore, studies have performed to investigate the effect of pulsed charging by TENGs on the electrochemical properties of electrode materials and to search for efficient energy storage systems for TENGs. For the battery research community, utilizing different charging waveforms to improve the battery performances has already been investigated, such as square-wave-current charging (pulsed charging either with a certain rest time or with a reverse current) and sinusoidal-ripple-current charging.[116,117] Compared to the constant-current-charging mode, generally they have the following benefits: (i) the intermittent charging with certain period of rest or reverse current can suppress the local charge aggregation and lower the concentration polarization and (ii) the increasing temperature can be lowered due to the heat dissipation during the rest time. Therefore, it is reasonable to expect that charging electrochemical energy storage devices with TENGs is beneficial for their performances.

Pu *et al.* first demonstrated the efficient charging of LIBs with the pulsed output of a rotational TENG.[98] Compared to the charging by a constant current, charging $LiFePO_4$ and $Li_4Ti_5O_{12}$ half cells with the TENG for the same time period delivered slightly larger discharge capacities when being discharged at a rate of 0.5C. Later, similar characteristics were reported for Li–S batteries, Li-ion capacitors, flexible LIBs, Na-ion batteries and Zn–air batteries.[118–122] Nevertheless, Li *et al.* reported that the pulsed charging of LIBs is detrimental to their cycling performances due to the pulverization of the electrode particles.[123] Their simulation results showed that pulsed charging may lead to higher strain and more cracks in the electrode particles. However, for their experimental results, the comparison was not made based on the same current rates. The short-circuit current of the pulsed power source was recorded, rather than the current during real-time charging. Savoye *et al.* found that

Open Access Article. Published on 03 November 2020. Downloaded on 07.01.26 14:11:40.
This article is licensed under a Creative Commons Attribution-NonCommercial 3.0 Unported Licence.

periodic pulse charging is detrimental to the performances of LIB compared to constant-current charging based on an identical mean current.[124] However, Chen *et al.* reported that the charging efficiency, cycling performances and maximum temperature of the LIB were all improved with sinusoidal-ripple-current charging.[116] Therefore, the effect of the pulsed charging on LIBs is still in debate and requires more systematic research.

The beneficial effects of pulsed-current electroplating for Li metal electrodes have been reported by several different groups. Li *et al.* reported that the lifetime of a symmetric Li metal cell was more than doubled using a square-wave pulse current compared to the constant current mode.[125] Both their experimental and molecular dynamics simulation results demonstrated the effectiveness of the pulsed current in suppressing the dendrite growth of Li metal. Wang *et al.* further used a square-wave current with a certain period of reverse current (*i.e.* the asymmetrical bidirectional current), and found that the Li dendrites were better suppressed compressing to the constant-current mode and intermittent constant current mode (Fig. 6a).[126] This improvement is because new or mild dendrites can be corrected (or healed) by the reverse current. Qiu *et al.* found that the pulsed charging by a TENG can alleviate the dendrite growth of a solid-state Li metal battery.[127] Li ions can diffuse uniformly during the intermittent period of the pulse current, and the growth of the dendrites was inhibited. Their *in situ* microscopy observation also demonstrated the alleviated dendrite growth under pulsed current mode, as shown in Fig. 6b. Zhang *et al.* further demonstrated the effectiveness of the sinusoidal ripple current of a rotational TENG in suppressing the Li dendrite growth.[128] As shown in Fig. 6c, the rotational TENG could output a high-frequency sinusoidal ripple current, which helped the uniform deposition of Li metal and improved the cycling life of the Li metal batteries. They

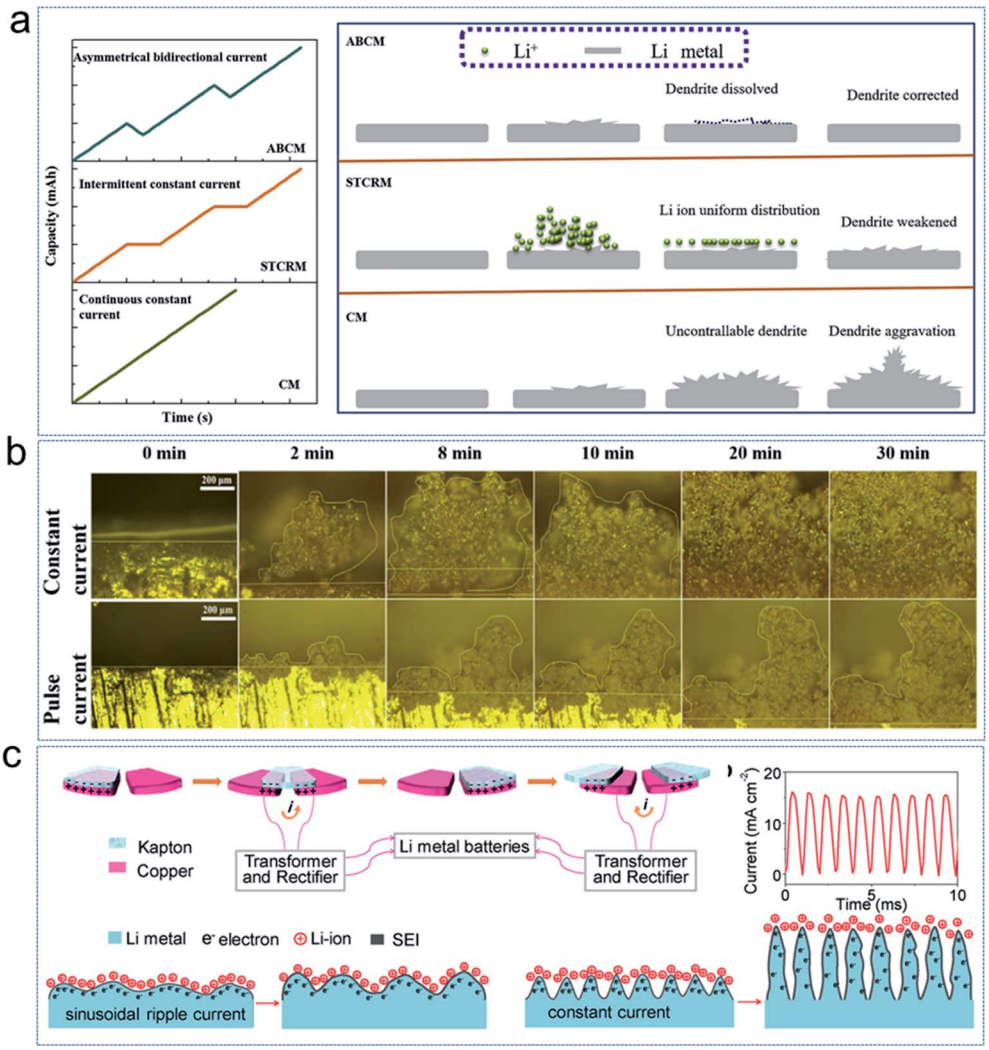

Fig. 6 Effects of pulsed charging on the Li metal electrodes. (a) Schematic comparison of the electrodeposition of Li metal using a constant current, intermittent constant current and intermittent asymmetric bidirectional current. Adapted from ref. 126 Copyright© 2020 Elsevier. (b) Real-time observation of the Li electrodeposition with pulse current and constant current. Adapted from ref. 127 Copyright© 2020 American Chemical Society. (c) Schematic comparison of the Li deposition using a constant current and sinusoidal ripple current generated by a rotating TENG. Adapted from ref. 128 Copyright© 2019 John Wiley & Sons, Inc.

© 2021 The Author(s). Published by the Royal Society of Chemistry

Open Access Article. Published on 03 November 2020. Downloaded on 07.01.26 14:11:40.
This article is licensed under a Creative Commons Attribution-NonCommercial 3.0 Unported Licence.

tested both the Li symmetric cells and an Li–$LiFePO_4$ cell. Compared to the constant-current mode, the sinusoidal ripple current of the TENG improved the cycling stability of the symmetric cell and the cycling capacity retention of the Li–$LiFePO_4$ cell.

When supercapacitors are utilized as the energy storage unit in SCPS, caution should be paid to another issue, *i.e.* their high self-discharge rate. Since the charging current of TENGs is relatively low and intermittent, it will take a longer time to charge a supercapacitor if its self-discharge rate is high. LIBs typically have low self-discharge rate, but supercapacitors, especially electric double layer capacitors (EDLCs) with aqueous electrolyte, have a high self-discharge rate. Xia *et al.* proposed a strategy to add the liquid crystal 4-*n*-pentyl-4′-cyanobiphenyl (5CB) in the electrolyte to suppress the self-discharge rate of the EDLC.[129] The aligned liquid crystal molecules increased the viscosity of the electrolyte in the charged state, leading to the suppression of self-discharge. Consequently, the EDLC with the modified electrolyte showed a higher charging efficiency when being charged by a TENG.

6. Prospects

In summary, the integration of mechanical energy harvesters (PENGs and/or TENGs) with energy storage devices into an SCPS provides a promising approach to achieve self-powered electronics, and exciting progress has been achieved recently. Different self-charging mechanisms have been proposed, such as the piezoelectric-potential-driven self-charging cells and integrated self-charging systems with external conditioning circuits. Various multi-functions have been realized in SCPSs, such as wearability, stretchability, transparency, and self-cleaning. The recent progress on power management circuits demonstrates the viability in filling the gap between the energy harvesting and storage devices in SCPSs, and in efficiently utilizing the harvested unstable energy for consistent power supply for electronics. Furthermore, preliminary understandings have been achieved on the unique characteristics of the pulsed charging process in SCPSs.

However, despite the progress, future research including the following aspects (Fig. 7) are still required to make TENG- or PENG-based SCPSs applicable for real applications:

(1) Performances

The output performances of TENGs and PENGs need to be improved. In the case of TENGs, the generated energy per motion cycle is calculated by the area of the *V*–*Q* plot.[105] The average energy will also be related to the motion frequency (*i.e.* the number of motion cycles per seconds). The key is to increase the transferred charge quantity, *Q*, which also determines the output voltage. Exciting progress has been made recently that the transferred charge quantity per motion cycle can reach 2.38 mC m^{-2} through a charge pumping approach.[130] By a rough

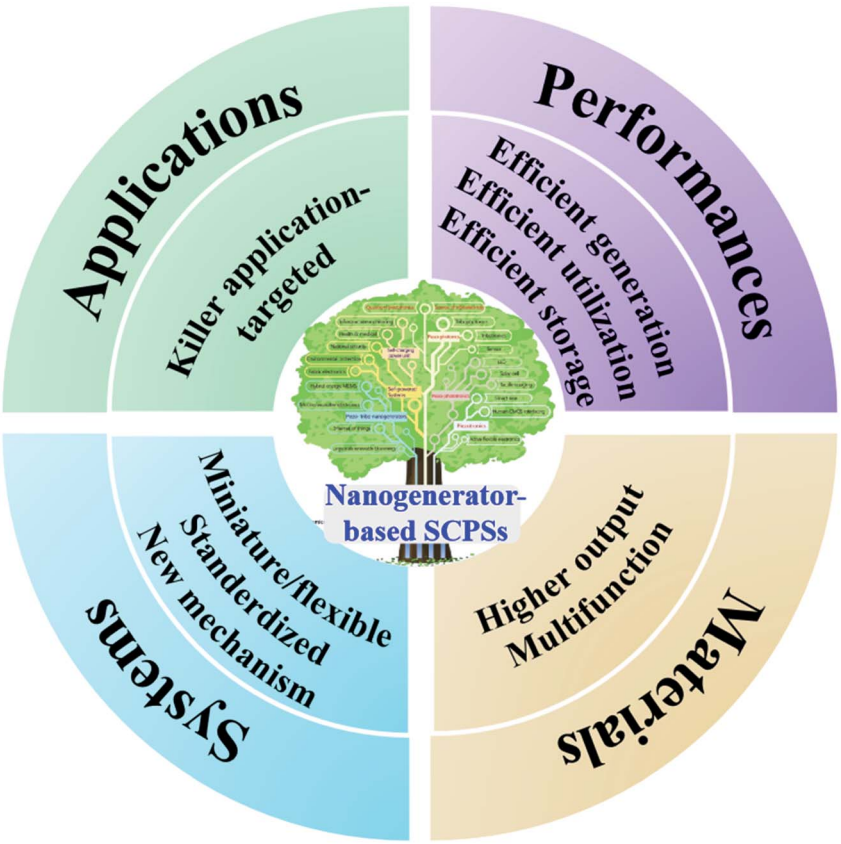

Fig. 7 Prospects of nanogenerator-based SCPSs.

Open Access Article. Published on 03 November 2020. Downloaded on 07.01.26 14:11:40.
This article is licensed under a Creative Commons Attribution-NonCommercial 3.0 Unported Licence.

estimation, the average maximum power density can be at a level of several watts per square meter, given the motion frequency is 1 Hz, which is already enough for powering many electronics even with wireless communications. Further improvements of the performances are expected, and future studies are needed to integrate these methods into self-charging systems.

The power management circuit is another key factor for the total power performances of SCPSs. As one aspect, the half-wave rectifying circuit, Bennet's doubler conditioning circuit, and charge pumping circuit have been demonstrated to improve the output of TENGs.[103] In another aspect, the power utilization efficiency can be improved to increase the total performances of SCPSs. The pre-requisite of achieving high efficiency through the circuit is the high output voltage of the TENG, otherwise not much efficiency increase will be obtained from the step-down conversion. The switched capacitor circuit seems to be a straightforward and effective way for the step-down conversion,[115] but it may be difficult to achieve a miniature size if the number of capacitors is large. Also, future research is still needed to optimize the hysteresis switch to improve the energy utilization and the automation of the circuit.

In terms of energy storage devices, the following aspects need further investigation. Firstly, the self-discharging of supercapacitors must be further reduced, especially for EDL supercapacitors. The utilization of electrochemical energy storage devices with low self-discharge rates may be a better choice, such as aqueous batteries or LIBs. Secondly, their cycling life should be long considering the real application scenario of the SCPS. An alternative approach is to not charge–discharge the energy storage devices in their full range. For example, they are only cycled between 20–80% state of charge (SOC), thus their cycling life can be prolonged. Accordingly, this also requires the design of the power management circuit. Currently, the research on SCPSs reached this far, and thus future studies are required.

Another issue for future research is to unify the performance standards of SCPSs. The charging efficiency and charge storing rate may be of both prime importance. Therefore, the literature can be better compared and the progress of this field can be promoted. The charge storing rate can be easily determined. The evaluation of charging efficiency should be unified in the future.

(2) Materials

From the perspective of materials studies, it is suggested that attention be given to the following aspects. Firstly, the materials studies for the improvement of the outputs of the TENGs or PENGs. Tuning the electrification properties of dielectric materials can be an effective approach through surface modification,[131] functional groups in the polymer chains,[132] ionic doping,[133] and embedded polarized layers.[134] Secondly, materials studies are the key to achieve multi-functionalities in SCPSs. Studies are required for not only multifunctional materials and both electrodes and electrification materials, but also their cooperative integration to overcome their incompatibility and interface issues. Furthermore, there will be bigger challenges to achieve multifunction of the whole SCPS if all the integrated parts of the system are considered. Thirdly, it seems that there is still no conclusive agreement on the effect of pulsed charging by TENGs on the performances of batteries; on the contrary, its beneficial effects on suppressing the dendrite growth of metal electrodes have been accepted.

(3) Systems

The following challenges remain to be addressed for the system integration of SCPSs. Firstly, the core challenges are still mainly related to the power management circuits. Since the circuit is hard to be flexible or stretchable, it is better to be miniature in size for wearable applications. If only diodes and capacitors are used (in the case of using diodes for rectifying and SCC for step-down conversion), it is still possible to achieve a flexible circuit in the future. Secondly, each part of the SCPS has to be designed according to specifically determined standards to achieve SCPSs integrated *via* mass production. For example, the parameters of the capacitors in the circuit have to be determined according to the output of the TENG so that the efficiency can be maximized, which means specific standards should be set for the TENGs, circuit and storage devices, otherwise mass production with comparable performances will be impossible. Thirdly, DC electricity nanogenerators with new mechanisms based on triboelectric or piezoelectric effects are highly expected to lower the complexity of systems, for example, the recently reported tribo-discharge-based DC nanogenerator[47] and tribovoltaic DC nanogenerator.[135]

(4) Applications

The last step for the success of SCPSs is to find their ultimate applications, where other competing technologies are not effective or applicable. The core advantages of the TENG-based SCPSs include high efficiency at low frequency and at small motion impact or amplitudes, and versatility in realizing multifunctionalities due to the vast materials choices. Meantime, they are less affected by the weather, time, and location compared to solar cells. These merits endow them with potential IoT applications, where power cables cannot be reached, and/or the electronic devices are not stationary, and/or multifunctionalities are required. Future research needs to be guided with certain targeted applications, which also requires the cooperation from industry.

All in all, fast development of this area and breakthroughs in real applications are highly expected in the near future, considering the exciting progresses have been made and great potentials have been demonstrated as discussed above.

Conflicts of interest

There are no conflicts to declare.

Acknowledgements

The authors thank for the support from the Youth Innovation Promotion Association of CAS.

© 2021 The Author(s). Published by the Royal Society of Chemistry

Open Access Article. Published on 03 November 2020. Downloaded on 07.01.26 14:11:40.
This article is licensed under a Creative Commons Attribution-NonCommercial 3.0 Unported Licence.

References

1 Z. L. Wang, *Mater. Today*, 2017, **20**, 74–82.
2 Z. L. Wang, *Nano Energy*, 2019, **58**, 669–672.
3 X. Pu, W. Hu and Z. L. Wang, *Small*, 2018, **14**, 1702817.
4 J. Kim, J. H. Lee, J. Lee, Y. Yamauchi, C. H. Choi and J. H. Kim, *APL Mater.*, 2017, **5**, 073804.
5 J. Luo and Z. L. Wang, *Energy Storage Materials*, 2019, **23**, 617–628.
6 K. Zhao, Y. Wang, L. Han, Y. Wang, X. Luo, Z. Zhang and Y. Yang, *Nano-Micro Lett.*, 2019, **11**, 19.
7 Z. L. Wang and J. Song, *Science*, 2006, **312**, 242–246.
8 Z. L. Wang, *Sci. Am.*, 2008, **298**, 82–87.
9 G. Zhu, R. Yang, S. Wang and Z. L. Wang, *Nano Lett.*, 2010, **10**, 3151–3155.
10 J. Bae, Y. J. Park, M. Lee, S. N. Cha, Y. J. Choi, C. S. Lee, J. M. Kim and Z. L. Wang, *Adv. Mater.*, 2011, **23**, 3446–3449.
11 Y. Hu, Y. Zhang, C. Xu, L. Lin, R. L. Snyder and Z. L. Wang, *Nano Lett.*, 2011, **11**, 2572–2577.
12 X. Y. Xue, S. H. Wang, W. X. Guo, Y. Zhang and Z. L. Wang, *Nano Lett.*, 2012, **12**, 5048–5054.
13 F. R. Fan, Z. Q. Tian and Z. L. Wang, *Nano Energy*, 2012, **1**, 328–334.
14 Z. L. Wang, *ACS Nano*, 2013, **7**, 9533–9557.
15 Z. L. Wang, *Nano Energy*, 2020, **68**, 104272.
16 X. Xiao, T. Li, P. Yang, Y. Gao, H. Jin, W. Ni, W. Zhan, X. Zhang, Y. Cao, J. Zhong, L. Gong, W. C. Yen, W. Mai, J. Chen, K. Huo, Y. L. Chueh, Z. L. Wang and J. Zhou, *ACS Nano*, 2012, **6**, 9200–9206.
17 S. Wang, Z. H. Lin, S. Niu, L. Lin, Y. Xie, K. C. Pradel and Z. L. Wang, *ACS Nano*, 2013, **7**, 11263–11271.
18 X. Pu, L. Li, H. Song, C. Du, Z. Zhao, C. Jiang, G. Cao, W. Hu and Z. L. Wang, *Adv. Mater.*, 2015, **27**, 2472–2478.
19 L. Xing, Y. Nie, X. Xue and Y. Zhang, *Nano Energy*, 2014, **10**, 44–52.
20 Y. S. Kim, Y. Xie, X. Wen, S. Wang, S. J. Kim, H. K. Song and Z. L. Wang, *Nano Energy*, 2015, **14**, 77–86.
21 X. Y. Xue, P. Deng, B. He, Y. X. Nie, L. L. Xing, Y. Zhang and Z. L. Wang, *Adv. Energy Mater.*, 2014, **4**, 1301329.
22 E. Jacques, G. Lindbergh, D. Zenkert, S. Leijonmarck and M. H. Kjell, *ACS Appl. Mater. Interfaces*, 2015, **7**, 13898–13904.
23 D. Zhou, N. Wang, T. Yang, L. Wang, X. Cao and Z. L. Wang, *Mater. Horiz.*, 2020, **7**, 2158–2167.
24 Y. Zhan, Y. Zhang, X. Xue, C. Cui, B. He, Y. Nie, P. Deng and Z. L. Wang, *Nanotechnology*, 2014, **25**, 105401.
25 D. Zhou, L. Xue, L. Wang, N. Wang, W. M. Lau and X. Cao, *Nano Energy*, 2019, **61**, 435–441.
26 P. Pazhamalai, K. Krishnamoorthy, V. K. Mariappan, S. Sahoo, S. Manoharan and S. J. Kim, *Adv. Mater. Interfaces*, 2018, **5**, 1800055.
27 G. Wei, Z. Wang, R. Zhu and H. Kimura, *J. Electrochem. Soc.*, 2018, **165**, A1238–A1246.
28 P. Thakur, A. Kool, N. A. Hoque, B. Bagchi, F. Khatun, P. Biswas, D. Brahma, S. Roy, S. Banerjee and S. Das, *Nano Energy*, 2018, **44**, 456–467.
29 F. Wang, C. Jiang, C. Tang, S. Bi, Q. Wang, D. Du and J. Song, *Nano Energy*, 2016, **21**, 209–216.
30 A. Rasheed, W. He, Y. Qian, H. Park and D. J. Kang, *ACS Appl. Mater. Interfaces*, 2020, **12**, 20891–20900.
31 A. Maitra, S. K. Karan, S. Paria, A. K. Das, R. Bera, L. Halder, S. K. Si, A. Bera and B. B. Khatua, *Nano Energy*, 2017, **40**, 633–645.
32 H. He, Y. Fu, T. Zhao, X. Gao, L. Xing, Y. Zhang and X. Xue, *Nano Energy*, 2017, **39**, 590–600.
33 R. Song, H. Jin, X. Li, L. Fei, Y. Zhao, H. Huang, H. Lai-Wa Chan, Y. Wang and Y. Chai, *J. Mater. Chem. A*, 2015, **3**, 14963–14970.
34 K. Parida, V. Bhavanasi, V. Kumar, J. Wang and P. S. Lee, *J. Power Sources*, 2017, **342**, 70–78.
35 E. P. Gilshteyn, D. Amanbaev, M. V. Silibin, A. Sysa, V. A. Kondrashov, A. S. Anisimov, T. Kallio and A. G. Nasibulin, *Nanotechnol*, 2018, **29**, 325501.
36 S. Sahoo, K. Krishnamoorthy, P. Pazhamalai, V. K. Mariappan, S. Manoharan and S. J. Kim, *J. Mater. Chem. A*, 2019, **7**, 21693–21703.
37 D. Zhou, N. Wang, T. Yang, L. Wang, X. Cao and Z. L. Wang, *Mater. Horiz.*, 2020, **7**, 2158–2167.
38 N. Wang, W. Dou, S. Hao, Y. Cheng, D. Zhou, X. Huang, C. Jiang and X. Cao, *Nano Energy*, 2019, **56**, 868–874.
39 A. Ramadoss, B. Saravanakumar, S. W. Lee, Y. S. Kim, S. J. Kim and Z. L. Wang, *ACS Nano*, 2015, **9**, 4337–4345.
40 K. Krishnamoorthy, P. Pazhamalai, V. K. Mariappan, S. S. Nardekar, S. Sahoo and S. J. Kim, *Nat. Commun.*, 2020, **11**, 2351.
41 D. Zhou, F. Wang, J. Yang and L. Z. Fan, *Chem. Eng. J.*, 2021, **406**, 126825.
42 D. Zhou, F. Wang, X. Zhao, J. Yang, H. Lu, L. Y. Lin and L. Z. Fan, *ACS Appl. Mater. Interfaces*, 2020, **12**, 44883–44891.
43 Z. Wang, *ACS Appl. Mater. Interfaces*, 2017, **9**, 15893–15897.
44 L. Gu, J. Liu, N. Cui, Q. Xu, T. Du, L. Zhang, Z. Wang, C. Long and Y. Qin, *Nat. Commun.*, 2020, **11**, 1030.
45 Y. Yang, H. Zhang and Z. L. Wang, *Adv. Funct. Mater.*, 2014, **24**, 3745–3750.
46 C. Zhang, T. Zhou, W. Tang, C. Han, L. Zhang and Z. L. Wang, *Adv. Energy Mater.*, 2014, **4**, 1301798.
47 D. Liu, X. Yin, H. Guo, L. Zhou, X. Li, C. Zhang, J. Wang and Z. L. Wang, *Sci. Adv.*, 2019, **5**, eaav6437.
48 Z. L. Wang, *Faraday Discuss.*, 2014, **176**, 447–458.
49 C. Wu, A. C. Wang, W. Ding, H. Guo and Z. L. Wang, *Adv. Energy Mater.*, 2019, **9**, 1802906.
50 J. Nie, X. Chen and Z. L. Wang, *Adv. Funct. Mater.*, 2019, **29**, 1806351.
51 X. Pu, L. Li, M. Liu, C. Jiang, C. Du, Z. Zhao, W. Hu and Z. L. Wang, *Adv. Mater.*, 2016, **28**, 98–105.
52 J. Wang, X. Li, Y. Zi, S. Wang, Z. Li, L. Zheng, F. Yi, S. Li and Z. L. Wang, *Adv. Mater.*, 2015, **27**, 4830–4836.
53 K. Dong, Y. C. Wang, J. Deng, Y. Dai, S. L. Zhang, H. Zou, B. Gu, B. Sun and Z. L. Wang, *ACS Nano*, 2017, **11**, 9490–9499.
54 Y. Song, J. Zhang, H. Guo, X. Chen, Z. Su, H. Chen, X. Cheng and H. Zhang, *Appl. Phys. Lett.*, 2017, **111**, 073901.

© 2021 The Author(s). Published by the Royal Society of Chemistry

Open Access Article. Published on 03 November 2020. Downloaded on 07.01.26 14:11:40.
This article is licensed under a Creative Commons Attribution-NonCommercial 3.0 Unported Licence.

55 J. Chen, H. Guo, X. Pu, X. Wang, Y. Xi and C. Hu, *Nano Energy*, 2018, **50**, 536–543.
56 M. Liu, Z. Cong, X. Pu, W. Guo, T. Liu, M. Li, Y. Zhang, W. Hu and Z. L. Wang, *Adv. Funct. Mater.*, 2019, **29**, 1806298.
57 Z. Cong, W. Guo, Z. Guo, Y. Chen, M. Liu, T. Hou, X. Pu, W. Hu and Z. L. Wang, *ACS Nano*, 2020, **14**, 5590–5599.
58 Y. Yang, L. Xie, Z. Wen, C. Chen, X. Chen, A. Wei, P. Cheng, X. Xie and X. Sun, *ACS Appl. Mater. Interfaces*, 2018, **10**, 42356–42362.
59 J. Zhao, H. Li, C. Li, Q. Zhang, J. Sun, X. Wang, J. Guo, L. Xie, J. Xie, B. He, Z. Zhou, C. Lu, W. Lu, G. Zhu and Y. Yao, *Nano Energy*, 2018, **45**, 420–431.
60 Y. C. Lai, J. Deng, S. L. Zhang, S. Niu, H. Guo and Z. L. Wang, *Adv. Funct. Mater.*, 2017, **27**, 1604462.
61 Y. Song, X. Cheng, H. Chen, J. Huang, X. Chen, M. Han, Z. Su, B. Meng, Z. Song and H. Zhang, *J. Mater. Chem. A*, 2016, **4**, 14298–14306.
62 N. Sun, Z. Wen, F. Zhao, Y. Yang, H. Shao, C. Zhou, Q. Shen, K. Feng, M. Peng, Y. Li and X. Sun, *Nano Energy*, 2017, **38**, 210–217.
63 H. Guo, M. H. Yeh, Y. Zi, Z. Wen, J. Chen, G. Liu, C. Hu and Z. L. Wang, *ACS Nano*, 2017, **11**, 4475–4482.
64 X. Shi, S. Chen, H. Zhang, J. Jiang, Z. Ma and S. Gong, *ACS Sustainable Chem. Eng.*, 2019, **7**, 18657–18666.
65 C. Zhou, Y. Yang, N. Sun, Z. Wen, P. Cheng, X. Xie, H. Shao, Q. Shen, X. Chen, Y. Liu, Z. L. Wang and X. Sun, *Nano Res.*, 2018, **11**, 4313–4322.
66 J. Wang, Z. Wen, Y. Zi, P. Zhou, J. Lin, H. Guo, Y. Xu and Z. L. Wang, *Adv. Funct. Mater.*, 2016, **26**, 1070–1076.
67 F. Yi, J. Wang, X. Wang, S. Niu, S. Li, Q. Liao, Y. Xu, Z. You, Y. Zhang and Z. L. Wang, *ACS Nano*, 2016, **10**, 6519–6525.
68 J. Shi, X. Chen, G. Li, N. Sun, H. Jiang, D. Bao, L. Xie, M. Peng, Y. Liu, Z. Wen and X. Sun, *Nanoscale*, 2019, **11**, 7513–7519.
69 X. Wang, Y. Yin, F. Yi, K. Dai, S. Niu, Y. Han, Y. Zhang and Z. You, *Nano Energy*, 2017, **39**, 429–436.
70 J. Luo, W. Tang, F. R. Fan, C. Liu, Y. Pang, G. Cao and Z. L. Wang, *ACS Nano*, 2016, **10**, 8078–8086.
71 S. Chun, W. Son, G. Lee, S. H. Kim, J. W. Park, S. J. Kim, C. Pang and C. Choi, *ACS Appl. Mater. Interfaces*, 2019, **11**, 9301–9308.
72 H. Guo, M. H. Yeh, Y. C. Lai, Y. Zi, C. Wu, Z. Wen, C. Hu and Z. L. Wang, *ACS Nano*, 2016, **10**, 10580–10588.
73 K. Zhao, Q. Qin, H. Wang, Y. Yang, J. Yan and X. Jiang, *Nano Energy*, 2017, **36**, 30–37.
74 A. Maitra, S. Paria, S. K. Karan, R. Bera, A. Bera, A. K. Das, S. K. Si, L. Halder, A. De and B. B. Khatua, *ACS Appl. Mater. Interfaces*, 2019, **11**, 5022–5036.
75 W. Xiong, K. Hu, Z. Li, Y. Jiang, Z. Li, Z. Li and X. Wang, *Nano Energy*, 2019, **66**, 104149.
76 V. K. Mariappan, K. Krishnamoorthy, P. Pazhamalai, S. Natarajan, S. Sahoo, S. S. Nardekar and S. J. Kim, *Nano Energy*, 2020, **77**, 105248.
77 Q. Jiang, C. Wu, Z. Wang, A. C. Wang, J. H. He, Z. L. Wang and H. N. Alshareef, *Nano Energy*, 2018, **45**, 266–272.
78 Y. Song, H. Wang, X. Cheng, G. Li, X. Chen, H. Chen, L. Miao, X. Zhang and H. Zhang, *Nano Energy*, 2019, **55**, 29–36.
79 S. L. Zhang, Q. Jiang, Z. Wu, W. Ding, L. Zhang, H. N. Alshareef and Z. L. Wang, *Adv. Energy Mater.*, 2019, **9**, 1900152.
80 Q. Zhang, Q. Liang, Q. Liao, M. Ma, F. Gao, X. Zhao, Y. Song, L. Song, X. Xun and Y. Zhang, *Adv. Funct. Mater.*, 2018, **28**, 1803117.
81 T. Gao, K. Zhao, X. Liu and Y. Yang, *Nano Energy*, 2017, **41**, 210–216.
82 K. Zhao, Y. Yang, X. Liu and Z. L. Wang, *Adv. Energy Mater.*, 2017, **7**, 1700103.
83 X. Liu, K. Zhao, Z. L. Wang and Y. Yang, *Adv. Energy Mater.*, 2017, **7**, 1701629.
84 Y. Yang and Z. L. Wang, *Nano Energy*, 2015, **14**, 245–256.
85 Z. Wen, H. Guo, Y. Zi, M. H. Yeh, X. Wang, J. Deng, J. Wang, S. Li, C. Hu and L. Zhu, *ACS Nano*, 2016, **10**, 6526–6534.
86 H. Shao, P. Cheng, R. Chen, L. Xie, N. Sun, Q. Shen, X. Chen, Q. Zhu, Y. Zhang, Y. Liu, Z. Wen and X. Sun, *Nano-Micro Lett.*, 2018, **10**, 54.
87 C. Pan, W. Guo, L. Dong, G. Zhu and Z. L. Wang, *Adv. Mater.*, 2012, **24**, 3356–3361.
88 Y. Yang, H. Zhang, G. Zhu, S. Lee, Z.-H. Lin and Z. L. Wang, *ACS Nano*, 2013, **7**, 785–790.
89 Y. Yang, H. Zhang, Z.-H. Lin, Y. Liu, J. Chen, Z. Lin, Y. S. Zhou, C. P. Wong and Z. L. Wang, *Energy Environ. Sci.*, 2013, **6**, 2429–2434.
90 S. Wang, Z. L. Wang and Y. Yang, *Adv. Mater.*, 2016, **28**, 2881–2887.
91 Q. Jiang, B. Chen and Y. Yang, *ACS Appl. Energy Mater.*, 2018, **1**, 4269–4276.
92 Y. Jiang, Y. Wang, H. Wu, Y. Wang, R. Zhang, H. Olin and Y. Yang, *Nano-Micro Lett.*, 2019, **11**, 99.
93 H. Li, X. Zhang, L. Zhao, D. Jiang, L. Xu, Z. Liu, Y. Wu, K. Hu, M. R. Zhang, J. Wang, Y. Fan and Z. Li, *Nano-Micro Lett.*, 2020, **12**, 50.
94 S. Qin, Q. Zhang, X. Yang, M. Liu, Q. Sun and Z. L. Wang, *Adv. Energy Mater.*, 2018, **8**, 1800069.
95 Z. Wen, M. H. Yeh, H. Guo, J. Wang, Y. Zi, W. Xu, J. Deng, L. Zhu, X. Wang, C. Hu, L. Zhu, X. Sun and Z. L. Wang, *Sci. Adv.*, 2016, **2**, e1600097.
96 J. Chen, Y. Huang, N. Zhang, H. Zou, R. Liu, C. Tao, X. Fan and Z. L. Wang, *Nat. Energy*, 2016, **1**, 16138.
97 X. Pu, W. Song, M. Liu, C. Sun, C. Du, C. Jiang, X. Huang, D. Zou, W. Hu and Z. L. Wang, *Adv. Energy Mater.*, 2016, **6**, 1601048.
98 X. Pu, M. Liu, L. Li, C. Zhang, Y. Pang, C. Jiang, L. Shao, W. Hu and Z. L. Wang, *Adv. Sci.*, 2016, **3**, 1500255.
99 W. Liu, Z. Wang, G. Wang, G. Liu, J. Chen, X. Pu, Y. Xi, X. Wang, H. Guo, C. Hu and Z. L. Wang, *Nat. Commun.*, 2019, **10**, 1426.
100 L. Xu, T. Z. Bu, X. D. Yang, C. Zhang and Z. L. Wang, *Nano Energy*, 2018, **49**, 625–633.
101 X. Cheng, W. Tang, Y. Song, H. Chen, H. Zhang and Z. L. Wang, *Nano Energy*, 2019, **61**, 517–532.

© 2021 The Author(s). Published by the Royal Society of Chemistry

Open Access Article. Published on 03 November 2020. Downloaded on 07.01.26 14:11:40.
This article is licensed under a Creative Commons Attribution-NonCommercial 3.0 Unported Licence.

102 S. Xu, L. Zhang, W. Ding, H. Guo, X. Wang and Z. L. Wang, *Nano Energy*, 2019, **66**, 104165.
103 A. Ghaffarinejad, J. Y. Hasani, R. Hinchet, Y. Lu, H. Zhang, A. Karami, D. Galayko, S. W. Kim and P. Basset, *Nano Energy*, 2018, **51**, 173–184.
104 L. Xu, H. Wu, G. Yao, L. Chen, X. Yang, B. Chen, X. Huang, W. Zhong, X. Chen, Z. Yin and Z. L. Wang, *ACS Nano*, 2018, **12**, 10262–10271.
105 Y. Zi, S. Niu, J. Wang, Z. Wen, W. Tang and Z. L. Wang, *Nat. Commun.*, 2015, **6**, 8376.
106 Y. Zi, J. Wang, S. Wang, S. Li, Z. Wen, H. Guo and Z. L. Wang, *Nat. Commun.*, 2016, **7**, 10987.
107 G. Cheng, H. Zheng, F. Yang, L. Zhao, M. Zheng, J. Yang, H. Qin, Z. Du and Z. L. Wang, *Nano Energy*, 2018, **44**, 208–216.
108 H. Zhang, F. Marty, X. Xia, Y. Zi, T. Bourouina, D. Galayko and P. Basset, *Nat. Commun.*, 2020, **11**, 3221.
109 F. Xi, Y. Pang, W. Li, T. Jiang, L. Zhang, T. Guo, G. Liu, C. Zhang and Z. L. Wang, *Nano Energy*, 2017, **37**, 168–176.
110 S. Niu, X. Wang, F. Yi, Y. S. Zhou and Z. L. Wang, *Nat. Commun.*, 2015, **6**, 8975.
111 X. Cheng, L. Miao, Y. Song, Z. Su, H. Chen, X. Chen, J. Zhang and H. Zhang, *Nano Energy*, 2017, **38**, 438–446.
112 W. Harmon, D. Bamgboje, H. Guo, T. Hu and Z. L. Wang, *Nano Energy*, 2020, **71**, 104642.
113 Y. Zi, H. Guo, J. Wang, Z. Wen, S. Li, C. Hu and Z. L. Wang, *Nano Energy*, 2017, **31**, 302–310.
114 W. Tang, T. Zhou, C. Zhang, F. Ru Fan, C. Bao Han and Z. Lin Wang, *Nanotechnol*, 2014, **25**, 225402.
115 W. Liu, Z. Wang, G. Wang, Q. Zeng, W. He, L. Liu, X. Wang, Y. Xi, H. Guo, C. Hu and Z. L. Wang, *Nat. Commun.*, 2020, **11**, 1883.
116 L. Chen, S. Wu, D. Shieh and T. Chen, *IEEE Trans. Ind. Electron.*, 2013, **60**, 88–97.
117 X. Huang, Y. Li, A. B. Achaya, X. Sui, J. Meng, R. Teodorescu and D. l. Store, *Energies*, 2020, **13**, 2458.
118 W. Song, C. Wang, B. Gan, M. Liu, J. Zhu, X. Nan, N. Chen, C. Sun and J. Chen, *Sci. Rep.*, 2017, **7**, 425.
119 H. Hou, Q. Xu, Y. Pang, L. Li, J. Wang, C. Zhang and C. Sun, *Adv. Sci.*, 2017, **4**, 1700072.
120 X. Liang, R. Qi, M. Zhao, Z. Zhang, M. Liu, X. Pu, Z. L. Wang and X. Lu, *Energy Storage Materials*, 2020, **24**, 297–303.
121 S. Li, D. Zhang, X. Meng, Q. A. Huang, C. Sun and Z. L. Wang, *Energy Storage Materials*, 2018, **12**, 17–22.
122 J. Bian, X. Cheng, X. Meng, J. Wang, J. Zhou, S. Li, Y. Zhang and C. Sun, *ACS Appl. Energy Mater.*, 2019, **2**, 2296–2304.
123 S. Li, Q. Wu, D. Zhang, Z. Liu, Y. He, Z. L. Wang and C. Sun, *Nano Energy*, 2019, **56**, 555–562.
124 F. Savoye, P. Venet, M. Millet and J. Groot, *IEEE Trans. Ind. Electron.*, 2012, **59**, 3481–3488.
125 Q. Li, S. Tan, L. Li, Y. Lu and Y. He, *Sci. Adv.*, 2017, **3**, e1701246.
126 D. Wang, C. Qin, X. Li, G. Song, Y. Liu, M. Cao, L. Huang and Y. Wu, *iScience*, 2020, **23**, 100781.
127 G. Qiu, L. Lu, Y. Lu and C. Sun, *ACS Appl. Mater. Interfaces*, 2020, **12**, 28345–28350.
128 Z. Zhang, Z. L. Wang and X. Lu, *Adv. Energy Mater.*, 2019, **9**, 1900487.
129 M. Xia, J. Nie, Z. Zhang, X. Lu and Z. L. Wang, *Nano Energy*, 2018, **47**, 43–50.
130 Y. Liu, W. Liu, Z. Wang, W. He, Q. Tang, Y. Xi, X. Wang, H. Guo and C. Hu, *Nat. Commun.*, 2020, **11**, 1599.
131 Y. Feng, Y. Zheng, S. Ma, D. Wang, F. Zhou and W. Liu, *Nano Energy*, 2016, **19**, 48–57.
132 S. Li, J. Nie, Y. Shi, X. Tao, F. Wang, J. Tian, S. Lin, X. Chen and Z. L. Wang, *Adv. Mater.*, 2020, **32**, 2001307.
133 H. Ryu, J. H. Lee, T. Y. Kim, U. Khan, J. H. Lee, S. S. Kwak, H. J. Yoon and S. W. Kim, *Adv. Energy Mater.*, 2017, **7**, 1700289.
134 J. Wang, C. Wu, Y. Dai, Z. Zhao, A. Wang, T. Zhang and Z. L. Wang, *Nat. Commun.*, 2017, **8**, 88.
135 Z. Zhang, D. Jiang, J. Zhao, G. Liu, T. Bu, C. Zhang and Z. L. Wang, *Adv. Energy Mater.*, 2020, **10**, 1903713.

© 2021 The Author(s). Published by the Royal Society of Chemistry